EFDA–JET–PR(14)11

S. Brezinsek, M.F. Stamp, D. Nishijima, D. Borodin, S. Devaux, K. Krieger,
S. Marsen, M. O'Mullane, C. Bjoerkas, A. Kirschner
and JET EFDA contributors

Study of Physical and Chemical Assisted Physical Sputtering of Beryllium in the JET ITER-Like Wall

Study of Physical and Chemical Assisted Physical Sputtering of Beryllium in the JET ITER-Like Wall

S. Brezinsek[1], M.F. Stamp[2], D. Nishijima[3], D. Borodin[1], S. Devaux[4], K. Krieger,[4]
S. Marsen[4], M. O'Mullane[2], C. Bjoerkas[5], A. Kirschner[1]
and JET EFDA contributors*

JET-EFDA, Culham Science Centre, OX14 3DB, Abingdon, UK

[1]Forschungszentrum Jülich GmbH, Association EURATOM-FZ Jülich, Institut für Plasmaphysik, Trilateral Euregio Cluster, D-52425 Jülich, Germany
[2]EURATOM-CCFE Fusion Association, Culham Science Centre, OX14 3DB, Abingdon, OXON, UK
3Center for Energy Research, University of California at San Diego, 9500 Gilman Drive, La Jolla, CA 92093-0417, USA
[4]Max-Planck-Institut für Plasmaphysik, 85748 Garching, Germany
[5]Department of Physics, University of Helsinki, POB 43, 00014 Helsinki, Finland
** See annex of F. Romanelli et al, "Overview of JET Results", (24th IAEA Fusion Energy Conference, San Diego, USA (2012)).*

Preprint of Paper to be submitted for publication in
Nuclear Fusion

ABSTRACT:

The effective sputtering yield of Be (Y_{Be}^{tot}) was determined in-situ by emission spectroscopy of low ionising Be as function of the deuteron impact energy ($E_{in} = 25 - 175eV$) and Be surface temperature ($T_{surf} = 200°C - 520°C$) in limiter discharges carried out in the JET tokamak. Be self sputtering dominates the erosion at high impact energies ($E_{in} > 150eV$) and causes Y_{Be}^{tot} far beyond 1. Y_{Be}^{tot} drops to extremely low values, below 2%, at the accessible lowest impact energy ($E_{in} \simeq 25eV$) achievable in limiter configuration. At medium impact energies, $E_{in} = 75eV$, two contributors to the measured Y_{Be}^{tot} of 9% were identified: two third of the eroded Be originates from bare physical sputtering (Y_{Be}^{phys} and one third from chemical assisted physical sputtering (Y_{Be}^{chem}). The later mechanism has been clearly identified by the appearance of *BeD* A-X emission and quantified in cause of a temperature dependence at which the *BeD* practically vanishes at highest observed Be limiter temperatures. The recorded T_{surf} dependence, obtained in a series of 34 identical discharges with ratch-up of T_{surf} by plasma impact and inertial cooling after the discharge, revealed that the reduction of *BeD* is correlated with an increase of D_2 emission. The release mechanism of deuterium in the Be interaction layer is exchanged under otherwise constant recycling flux conditions at the limiter.

The reduction of Y_{Be}^{chem} with T_{surf} is also correlated to the reduction of the Be content in the core plasma providing information on the total source strength and Be screening. The chemical assisted physical sputtering, always present at the nominal limiter pre-heating temperature of $T_{surf} = 200°C$, is associated with an additional sputtering channel with respect to ordinary physical sputtering which is surface temperature independent. These JET experiments in limiter configuration are used to benchmark the ERO code and verify ITER first wall erosion prediction. The ERO code overestimates the observed Be sputtering in JET by a factor of about 2.5 which can be transferred to ITER predictions and prolong the expected lifetime of first wall elements.

1. INTRODUCTION

JET is equipped with a first wall material combination comparable to the ITER selection comprising beryllium (Be) in the main chamber and tungsten (W) in the divertor and some recessed wall areas [1]. Be is selected owing to its low atomic number, its low tritium retention and excellent getter properties, but material erosion limits the lifetime of plasma-facing components (PFCs) made of Be. Initial Be erosion modelling of the shaped ITER first wall modules located close to the separatrix [2] predicts high erosion rates and limited armour lifetime [3]. However, uncertainties in the modelling, in particular in the atomic data and sputtering yields, still exist and further benchmark under ITER-comparable tokamak conditions is required. With the present material selection in JET such benchmarks can be performed.

The ITER-Like Wall in JET (JET-ILW) demonstrated successful plasma operation [4], strong reduction of the C content by a factor 20, and high plasma purity ($Z_{eff} \simeq 1.2$) [5]. The predicted advantages concerning low tritium retention and oxygen gettering were experimentally confirmed by global gas balance studies [6] and optical spectroscopy [7]. All these measurements confirm that

Be is the main and dominant intrinsic impurity in limited and diverted plasmas with the JET-ILW. Equipped with its bulk Be limiters (fig 1), the JET-ILW allows dedicated study of Be erosion by optical emission spectroscopy and observation of various transitions of *BeI* (e.g. 457*nm*), *BeII* (e.g. 527*nm*) and the *BeD* $A^2\Pi \rightarrow X^2\Sigma^+$ band (band head at 497 – 500*nm*) [9] under different plasma conditions and surface temperatures [10]. The total Be sputtering consists of the bare physical sputtering [11] and the chemical assisted physical sputtering [12] – sometimes referred as swift chemical sputtering. However, the composition of the total sputtering, its dependence on the impact energy and temperature, the strength of the chemical assisted physical sputtering are not known for a high temperature plasma edge conditions as present in JET-ILW or in future ITER. Experimental input from JET is required to verify the sputtering and transport modelling Monte-Carlo code ERO applied to predict the lifetime of shaped ITER blanket modules [13].

Here, dedicated deuterium plasmas in limiter configuration have been used to vary systematically the local electron temperature (T_e) in the scrape-off layer (SOL), or better, scanning the impact energy of the impinging deuterons (E_{in}), as well as, to vary the PFC surface temperature (T_{surf}) by plasma impact as they are only inertially cooled. The increase of T_{surf} is expected to inhibit the sputtering channel via BeD which thermally decomposes at about 540*K* according to studies in PISCES [14]. Though these are dedicated experiments with variation of one single parameter, impact energy or surface temperature, with the residual plasma and geometry conditions unchanged, the measured Be sputtering yields represent effective yields as averaging of the observation volume, the limiter geometry and the corresponding plasma profile takes place. Nevertheless, clear identification and quantification of both contributors to the Be sputtering yield and their variation with these parameters was achieved.

Details about the experimental set-up and the plasma conditions of the two limiter experiments are given in section 2. The quantification of the two contributors to the Be sputtering yield is presented in section 3 and the variation of the effective yield with the local electron temperature is shown in section 4. The discussion section 5 deals with the physics mechanisms behind the two processes and discusses accompanied ERO modelling which has been benchmarked with the present data. General remarks concerning the Be source strength in JET in limiter magnetic configuration as well as the degree of Be erosion expected in ITER concludes this contribution.

2. EXPERIMENTAL SET-UP AND PLASMA CONDITIONS

Two dedicated experiments in limiter configuration with contact point on the poloidal limiters at the high field side (HFS) (figure 2a) were carried out in order to study the Be sputtering yield with respect to a) its composition related to chemical and physical sputtering (experiment I), and b) its dependence on the local electron temperature, respectively, the impact energy of the impinging deuterons (experiment II).

2.1 EXPERIMENT I

In experiment I, initially performed for a global gas balance study which is described in more detail in [6], 34 identical deuterium plasma discharges ($B_t = 2.5T$, $I_p = 2.0MA$, $Pin = 2.0MW$) had been executed consecutively with a typical discharge repetition rate of $20min$. Typical, global time traces for central electron temperature T_e^C, central density n_e^C, input P_{in} and radiated power P_{rad}, for the last discharge of the series are depicted in (figure 2b); the averaging window in the plateau phase of the HFS limited plasmas for analysis is indicated. The discharges showed high reproducibility and though the fuelling rate of deuterium was moderate ($\Gamma = 6 \times 10^{21} es^{-1}$) and the radiated fraction was low ($frad = 20\%$), no sign of W peaking in the core was observed. $Z_{eff} < 1.5$ was determined by the Be content induced by Be sputtering predominantly at the inboard Be limiters as discussed in further detail below. The local plasma conditions at the observation spot of the spectroscopic diagnostic system (Czerny Turner spectrometer, grating: $1200l/mm$, spectral coverage: $420nm$ – $610nm$, spectral resolution: $0.6nm$ FWHM, temporal resolution: $\Delta t = 50ms$) on the limiter with the line-of-sight depicted in figure 2a) which lays in the near SOL one tile below the contact point were determined in-situ by line ratio analysis of pairs of *BeII* lines and low-n deuterium Balmer lines. In fact the local electron temperature was deduced from the line ratio of the *BeII* transitions at $467nm$ (transition) and at $436nm$ (transition) which shows a strong dependence on T_e in the range of $1 - 50eV$, but is practically independent of n_e in the range of $5 \times 10^{17} - 1 \times 10^{20}\mathrm{m}^{-3}$ which covers the conditions present in the JET SOL and edge layer in limiter plasmas.

In figure 3a) the calculated line ratio of these two lines according to the ADAS data base [15] is depicted and the actual line ratio measured in experiment I is marked. Figure 3b) shows the corresponding photon flux time evolution during an early and late discharge of the series JET Pulse No. 82592 – 82626. Time traces of additional Be and D transitions discussed below are depicted too. All spectroscopic data has been averaged in the time window $t = 10s - 11$s in the density flat-top phase of the discharge. The *BeII* line ratio remained constant in the averaged phase of all plasmas executed in experiment I. The local temperature and density deduced from spectroscopy amounts $T_e = 15eV$ and $n_e = 6 \times 10^{18} m^{-3}$ averaged over the observation chord with an area of $0.011m^2$ at the limiter location (tile 7). These plasma parameters are in agreement with Langmuir probe data from probes embedded in tile 9 which is located poloidally in the same distance away from the plasma contact point but upwards (figure 2). Assuming electron and ion temperature in the SOL are comparable in the present conditions, the energy of deuterons can be estimated by approximately $E_{in} = 3_{kb}T_e + 2k_bT_i \simeq 5 \times T_e$ [16], therefore, the impact energy of the impinging deuterons can be derived in-situ by the local electron temperature.

A peak power flux density of $5\mathrm{MW}m^{-2}$ is deposited onto the high-field side Be limiter during the flat-top phase of the discharges in experiment I and induces a continuous heatup of the inertially cooled inner wall limiter tiles during the discharge (*cf* Be tile power handling [17]). The temporal evolution of the peak surface temperature measured by IR thermography on the inner wall limiter tile 7 during the second discharge of experiment I is shown in figure 4a); note that this is a net-

erosion zone and no surface layers are present which might affect the interpretation of experimental data. The plasma is limited in the early phase of the discharge ($t = 0 - 5s$) to the outer wall limiter. The temperature measured by IR thermography on the inner wall tile 7 in this time period reflects therefore the Be bulk temperature, referred as T_{base} below, which is almost in thermal equilibrium at the beginning of the discharge as confirmed by thermo-couples. The plasma discharges in experiment I were executed with a typical repetition rate of $20min$; figure 4b) shows the discharge-to-discharge evolution of T_{base} determined by the IR thermography when it was technically available. As it can be seen each plasma pulse in experiment I ratchets up the bulk limiter temperature (JET Pulse No. 82592 – 82601) until equilibrium is reached between heating and cooling (JET Pulse No. 82602 – 82626). Because of all plasma parameters remain constant in the series of discharges, experiment I provides a fine scan of the base temperature at the beginning of the discharge in the range between $200°C$ and $420°C$ of inner wall Be limiter tile 7 which is in view of the spectroscopic system (line-of-sight in figure 2a). The lower temperature limit is determined by the active heating of the JET first wall to $200°C$. The actual peak surface temperature T_{surf} during the plasma excursion rises during the discharge (figure 4a)) adding typically ΔT of about $80K - 120K$ at the sampling point (t = 10 – 11s) used for the optical spectroscopy; the maximum value of the surface temperature lays even higher at about $150K$ above the base temperature. It should be noted that this ΔT refers only to the peak value within the tile 7 surface from a complex temperature distribution as depicted in figure 4c) in the full 2D picture. As the optical spectroscopy observation chord includes a larger area than the peak spot, averaging takes place and we refer in the following to T_{base} as reference temperature which is closer to the actual averaged temperature of tile 7.

2.2 EXPERIMENT II

Experiment II aims in the study of the Be sputtering as function of the impact energy E_{in} of the deuterons, respectively, of the local temperature T_e and density n_e at the contact point under comparable limiter temperature conditions. Seven ohmic and high-field-side limited discharges ($B_t = 2.8T, I_p = 2.0MA$), timely separated in two bunches of discharges at different days, have been performed varying $T_e^C = 1.7 - 3.4keV$ and $n_e^C = 2.7 - 7.0 \times 10^{19} m^{-3}$ by solely deuterium fuelling. The global time traces of the discharges with lowest and highest fuelling are depicted in figure 5 showing the large variation in the density and simultaneously to an almost reciprocal plasma temperature change. The low fuelled discharges with the highest edge electron temperatures reach high Be impurity concentrations with Z_{eff} in the hottest plasma edge case of about 4 which indicates that strong Be self sputtering must take place leading to a Be-rich plasma. The corresponding local plasma conditions were determined in-situ by *BeII* spectroscopy averaged over the line-of-sight on the limiter applying the before described line-ratio technique.

The time between two individual discharges in one subset of discharges as well as the small number of consecutive discharges in limiter configuration in this experiment minimised a ratch-up of the limiter temperature from discharge to discharge. T_{surf} is in this case close to T_{base}, and both are close

to the bulk limiter temperature of $200°C$ achieved by active heating. The corresponding effective sputtering values averaged concerning the area of the line-of-sight on the limiter are therefore representative of the standard condition case; temperature variation from discharge to discharge is not considered in the analysis of this experiment. Initial results on the Be sputtering yield in connection with ERO modelling from a subset of data have been presented in [8].

3 CONTRIBUTORS TO THE TOTAL BE SPUTTERING YIELD

3.1 INTERPRETATION OF SPECTROSCOPIC BE AND D-CONTAINING EMISSION

The temporal evolution of the brightness of BeI , $BeII$, BeD, D_2, and $D\gamma$ from discharge to discharge at the averaging time window in each discharge at t = 10.0 – 11.0s is shown in figure 6a). The conversion into actual bulk Be tile temperature (T_{base} is depicted correspondingly in figure 6b) showing variations in the first nine discharges and reaching equilibrium at $T_{base} = 400°C$ with a surface temperature of $T_{surf} \simeq 520°C$ in the spectroscopic sampling window of the ninth discharge. The residual discharges are within the error bars identical and show the reproducibility of the conditions very well.

The increase of the surface temperature leads to a reduction of all photon fluxes related to Be whereas $D\gamma$ remains constant in all discharges, indicating both constant plasma conditions and identical impinging fluxes to the limiter as full recycling can be assumed. In the same way the BeD A-X band emission decreases, the fraction of observed D_2 d-a emission (non-diagonal Fulcher band emission integrated over 580.3 – 584.1nm) increases indicating a shift in the release mechanism of deuterium from the saturated top surface layers. Figure 7 shows the emission spectra of the involved atomic lines and molecular bands for the low and high limiter temperature case. Though not the whole ro-vibrational band in both cases is measured, but only a reference wavelength span, the photon fluxes are directly proportional to the particle flux as a) the ro-vibrational population temperature is not varying significantly with the change of the surface temperature and b) the wavelength span covers at least one complete vibrational transition. Detailed studies on the temperature dependence of the Fulcher-α band were done in limiter plasmas in TEXTOR under similar plasma conditions, but graphite surfaces confirming that the slight increase of the rotational population temperature according to the Boltzmann distribution would be covered [18]. With the previously discussed assumptions, one can conclude that the released deuterium molecular particle flux is doubled in the important discharge series (JET Pulse No. 82592 – 82601) in which the the BeD flux dropped down close to the detection level. Under the present high T_e conditions at the limiters, the destruction of D_2 occurs preferably by electron impact dissociation via the molecular ion D_2^+, which results in effectively one potential D atom capable to radiate a Balmer photon with the appropriate photon efficiency [18]. This should have resulted in an increase of the D_γ radiation as representative for the recycling flux, however, the recycling flux measured by D_γ is constant. In balance, we can conclude that a similar amount of deuterium atoms must result from the dissociation process of BeD or BeD_2 which starts from the surface. In principle, a full balance would be possible if the

complete molecular bands would have been measured and simulated, but this was not accessible with the applied diagnostic equipment.

The line emission resulting from the Be ion (here e.g. *BeII* at 527*nm*) is hereby representative for the total Be sputtering source, including bare physical sputtering and chemical assisted physical sputtering, and the band emission of BeD (*BeD* A-X band head 496.0*nm* to 499.4*nm*) is solely representative for the branch of sputtering related to chemical assisted physical sputtering. The line emission originating from the neutral Be atom (here e.g. *BeI* at 457*nm*) results from physical sputtering and the fraction of Be sputtering via BeD which dissociates via $BeD + e \rightarrow Be + D + \acute{e}$. Thus, the particle flux ratio of *BeI* to *BeII* even provides information on the dissociation chain as any number smaller than unity indicates that not all BeD delivers finally a Be which can potentially radiate with the corresponding photon efficiency. Moreover, the application of appropriate inverse photon efficiencies, so-called S/XB, for the *BeI* I 527nm line [15, 10] and the normalisation to the impinging ion flux, determined by Dγ and multiplied with the corresponding S/XB-value leads to the total Be sputtering yield $Y_{Be}^{tot} = Y_{Be}^{phys} + Y_{Be}^{chem}$.

3.2 THE COMPOSITION OF THE TOTAL BE SPUTTERING YIELD

In figure 8a), Y_{Be}^{tot} is shown as function of measured temperature of the observed Be tile T_{base} determined by IR-thermography. It should be again noted that T_{base} is measured at the actual break-down of the discharge and the incremental peak temperature ΔT increase by about 100K until the measurement window at $t = 10 - 11s$ is reached during the plasma discharge. This is however averaged over the observation spot. A clear linear drop of Y_{Be}^{tot} with increasing temperature can be seen in the first nine identical plasma discharges till the maximum reachable temperature of the Be tile of about $520°C$ at the sampling time window has been reached. This strong reduction in Y_{Be}^{tot} by 33% is caused by the reduction of Y_{Be}^{chem} which vanishes almost completely at the highest T_{base} according to the *BeD* emission described before. Therefore, we can conclude that for the given plasma conditions at the limiter, $T_e = 15eV$ and $n_e = 6 \times 10^{18} m^{-3}$, determined by local *BeII* and Balmer-line ratio analysis, about 1/3 of Y_{Be}^{tot} is originating from Y_{Be}^{chem} and 2/3 from regular physical sputtering Y_{Be}^{phys}. This composition is in good agreement with MD modelling predictions [20] for the BeD release at an impact energy of $75eV$ which we can assume for this experiment considering $T_e = T_i$.

From a comparable analysis using *BeI* at 457*nm* instead of *BeII*, we obtain a reduction of Y_{Be}^{tot} by 25%. As the Be^+ reflects the end product along the dissociation chain, we can conclude that the difference lays in the dissociation path and the *BeI* to *BeII* flux ratio reveals that the preferred dissociation path is via the molecule *BeD* (75%) and only about 25% is following the destruction in plasma via $BeD + e \rightarrow BeD^+ + e + \acute{e}$. Note, that a recombination of Be and D into the BeD molecule can be excluded at the high and fully ionising electron temperatures at the limiter contact point and the near SOL of JET.

Further information can be obtained by comparing the reduction of Y_{Be}^{tot} with the change of the core concentration c_{Be} (figure 8b)) deduced from Z_{eff} [3] (figure 8c): under otherwise constant plasma

conditions, c_{Be} drops in the same manner as Y_{Be}^{tot} with T_{base} by about 30%. Comparing the absolute values, the erosion yield corresponds to twice the concentration in the plasma which suggests an impurity screening of 50% and that the ratio between gross and net erosion is also a factor 2 as the limiters represent the only source of Be. Moreover, the interlink between Be source and Be core content under otherwise constant conditions, in particular identical impinging deuterium ion flux as reflected by the constant $D\gamma$ in figure 6, confirms the chemical assisted physical sputtering of Be represent an additional sputtering channel of Be under the given conditions. However, the measurement of *BeII* , thus the flux of Be ions, provides still the total flux of eroded Be but the interpretation as bare physical sputtering is incorrect as the chemical assisted physical sputtering provides an additional sputtering channel contributing to Be^+.

A potential impact of a thick co-deposited layer at the interaction location can be excluded. Figure. 9 shows the emission of the *BeD* A-X band and $D\gamma$ during the short limiter start-up phase in the three discharges prior and post the series of plasmas in experiment I. The local plasma conditions are slightly different as the recycling flux suggests, however, clearly the emission of BeD is detectable after experiment I. The local temperature of the limiter reflects in these discharges with short interaction time the temperature of the actively heated Be limiters $200\,°C$ as at the beginning of experiment I. The appearance of the *BeD* A-X emission is therefore clearly connected to a sputtering process of bare Be and not a thick co-deposited layer. Moreover, post-mortem analysis of comparable tiles confirm after extraction that the observed limiter tiles reflect net-erosion areas over the whole period of the campaign. This erosion is dominated by the limiter phase or limiter discharges similar to the ones discussed in this paper.

3.3 COMPARISON WITH THE COMPOSITION OF THE TOTAL C SPUTTERING YIELD

The impurity release behaviour is to a certain extent similar to the sputtering of carbon from graphite with observation of C^+ (*CII* emission), representing physical and chemical erosion, and CD (*CD* A-X band emission), reflecting solely the chemical erosion with predominantly methane release and break-up into CD [19]. Also the chemical sputtering of graphite vanishes at higher surface temperatures as measured in TEXTOR under comparable edge plasma conditions as in JET. However, the chemical sputtering process and the energy of the radicals produced is different in the case of Be and C, whereas the latter is thermally released. Moreover, at the low energy range, an energy threshold for Be sputtering of about $10eV$ has been calculated [20] which inhibits erosion by low energetic ions or even thermal atoms as it occurs in the case of C. Note that this fact has vital importance on the material migration behaviour in the JET-ILW as the Be erosion in the far-SOL, thus, the main chamber wall and the divertor, will be reduced in diverted magnetic configurations in comparison with JET-C. This can be already seen in the dramatic reduction of the primary C source in comparison with the Be in JET-ILW [5] as well as the initial post-mortem analysis studies of limiters and divertor plasma-facing components [21].

4. TOTAL BE SPUTTERING YIELD AS FUNCTION OF E_{IN}

Experiment (II) aims to determine the dependency of Y_{Be}^{tot} on E_{in} in the accessible range of limiter plasma conditions with the JET-ILW. As no direct measurement of the impact energy exists, we still assume the validity of $E_{in} \simeq 5 \times T_e$ over the full plasma parameter range. Figure 10 shows the measured total sputtering yield Y_{Be}^{tot} as function of the local T_e deduced from local spectroscopy discussed before. The measured T_e in the SOL varies between $5eV$ and $35eV$ and is inversely proportional to the central plasma density which has been varied in a controlled manner by deuterium fuelling ramps. Y_{Be}^{tot} increases moderately with impact energy from $T_e \simeq 5$eV up to about $T_e \simeq 30$eV which is in line with the increase of the physical sputtering process by deuterons. We observe the dominance of self-sputtering by impinging Be ions at $T_e > 30eV$ and, thus, $E_{in} > 150eV$ which compromises the definition of the yield and normalisation to the deuterium ion flux. The contribution of Be self-sputtering to the total sputtering decrease with lower electron temperature and higher electron density. It is in the normal operational window of JETILW baseline discharges with phases of magnetic limiter configuration (start-up, limiter flat-top, and ramp-down) and pure ohmic heating usually not of importance ($Z_{eff} < 1.8$) in comparison with the sputtering contribution determined by the impinging deuterons. Only in dedicated experiments like here described, the full operational window is explored with on purpose high electron temperatures to study in particular the sputtering yield or the power load to the limiters. At the lowest controlled accessible Te $\simeq$ 5eV in limiter configuration before MARFE formation and inner wall detachment occurs, still the corresponding impact energy of $E_{in} \simeq 25$eV is above the energetic threshold for sputtering. The measurements at lowest and highest T_{base} from experiment (I) are marked in figure 10; indicating the impact of Y_{Be}^{chem} at one particular T_e value. The measurement at cold limiter conditions at $E_{in} = 75eV$ fits excellent in the point band of experiment (II).

The measurement point at highest limiter temperature in experiment (I), thus, without chemical assisted physical sputtering is well below the measurements of experiment (II). This indicates the importance of the second sputtering channel in the overall Be erosion yield. The yellow marked area spans the set of ERO calculations of the Be erosion yield simulating the effective sputtering Be erosion yield for a synthetic spectroscopic diagnostic considering the same line-of-sight and plasma conditions as present in experiment II. The calculations are performed solely under the assumption of bare physical sputtering of Be by deuterium and Be self-sputtering. The upper boundary is given by the so-called ERO-max envelope of available experimental and calculated sputtering yields as input parameter as described in [8]. Correspondingly, the lower boundary is determined by the most optimistic set of available sputtering yield values. In order to achieve the match depicted in figure 10, the impinging ion flux, benchmarked by the measured $D\gamma$ photon flux, had to be reduced by a factor 2. Though a 50% surface coverage of the Be surface with deuterium was assumed in the ERO calculations, the process of chemical assisted physical sputtering was not yet included in the suite of atomic and molecular processes. Consideration of the process would increase further the discrepancy between modelling and experiment as it is indicated by the larger gap between the lowest envelope

of EROmin at $T_e = 15eV$ for the case of the almost bare physical sputtering measured at the high T_{base} of experiment I. In other words, even with the additional measured sputtering channel, the corrected ERO-min calculations simulating the experiment overestimate by about a factor 2.3. The discrepancy increases further at the low energy range where the corrected ERO-min lays outside of the measurements without consideration of a potential higher fraction of BeD contributing to the effective sputtering yield. The match is better with increasing importance of Be self sputtering. This indicates that the set of Be sputtering yields used in ERO-min at the lower energy range needs to be critically revisited. Additional benchmarks including the process of chemical assisted physical sputtering employing MD calculated Be sputtering yields by [20] are foreseen to benchmark the code further with JET-ILW experimental results.

The current experimental results provide only a single measurement of the composition of Y_{Be}^{tot} for the impinging energy of $E_{in} = 75eV$ as the experiment is costly in experimental time and relies on high repletion rate of discharges in JET-ILW to heat-up the limiter by plasma impact. It is expected that the composition of the contributors to Y_{Be}^{tot} will likely change [20] in the plasma parameter range covered in experiment II with a higher fraction of Y_{Be}^{chem} at lowest energies, representing the fist wall conditions in divertor plasmas, and negligible contribution at the high energetic range, representing low density conditions in plasma start-ups for advanced plasma scenarios. Apart from the energy dependence which favours bare physical sputtering at high impact energies and deeper penetrations of deuterons into the Be matrix, also the reservoir of available deuterium impinging the limiter surface reduces on cost of additional Be impinging flux. This self-amplified process is usually inhibited by sufficient high deuterium fuelling in JET discharges to protect the first wall from too high Be concentrations in the plasma which can subsequently cause W sputtering when the divertor coils are switched on and the significant flux of plasma and impurities are hitting the tungsten divertor target plates.

Finally, we need to stress that the discussed Be sputtering yields represent effective yields due to averaging over the observation area on the 3D-geometry of the Be limiter tile. Averaging of local plasma conditions (T_e, n_e, E_{in}), impact angles, and impinging fluxes within the observation chord takes place. However, the here discussed measurements provide a good data set to new benchmarks with the ERO code, including the chemical assisted Be sputtering. ERO treats the involved processes on the atomistic level and can disentangle the individual processes in order to make predictions in more complex geometries and conditions like in ITER.

5. DISCUSSION

The main information obtained in these experimental work can be summarised as follows: (i) the effective sputtering yield of Be as function of impact energy ($E_{in} = 25 - 175eV$) and surface temperature ($T_{surf} = 200°C - 500°C$) has been determined in limiter configuration in-situ by emission spectroscopy in JET. (ii) At a medium impact energy ($E_{in} = 75eV$) two contributors to the total effective Be sputtering yield were identified. Two third of the eroded Be originates from

bare physical sputtering and one third from chemical assisted physical sputtering which practically vanishes at high Be limiter temperatures ($T_{surf} > 520°C$). (iii) Be self sputtering dominates the erosion at high impact energies ($E_{in} > 150eV$) and causes effective yields far beyond 1 whereas the normalisation to the impinging ion flux to the limiter is no longer useful. (iv) The effective Be sputtering yield drops to extremely low values, below 2%, at the accessible lowest impact energy ($E_{in} \simeq 25eV$) achievable in limiter configuration in JET.

5.1 THE ROLE OF CHEMICAL ASSISTED PHYSICAL SPUTTERING IN THE OVERALL BE EROSION

Though no dedicated experiments at lower impact energies in JET exist, it is expected that the contribution of chemical assisted physical sputtering gains further importance as the emission of *BeD* from recessed main chamber wall cladding tiles in divertor configuration suggests. Indeed, both MD modelling [18] and experiments at PISCES-B [12] predict at impact energies $E_{in} < 50eV$, the dominance of the Be chemical assisted physical sputtering over the bare physical sputtering before an energetic threshold at about $E_{in} < 10eV$ inhibits further sputtering. The measured JET-ILW value for the amount of Be sputtered as BeD is depicted in figure 11 and shows good agreement with both MD modelling and the experimental PISCES-B data. The PISCES-B measurements suggest that sputtering at higher energies is mainly unaffected by chemical assisted physical sputtering and only bare physical sputtering is the origin of eroded Be. This corresponds at JET to the region where experimentally self sputtering starts to become the dominant process. Contrary, at low impact energies the release as molecular compound is dominant over the release as energetic Be atom by bare physical sputtering. However, the experiments, both in JET and PISCES-B, cannot exclude that the chemical assisted physical sputtering takes place with the release of the stable molecule BeD_2 rather than the radical BeD. There is no direct spectroscopic access to BeD_2 in the experiments.

The contribution of the molecular compounds of Be to the total sputtering yield of Be depends on the amount and form of D embedded in the Be surface layers within the ion implantation range. Without sufficient deuterium reservoir present, the release of chemical compounds by physical impact is much reduced which means independently of the destruction process of a BeD molecule, at higher surface temperatures and lower fuel content in the Be, less molecular-related sputtering can be expected. Here, the high impinging deuterium ion flux in limiter configuration, a few 10^{21} $Ds^{-1}m^{-2}$ and corresponding fluence per inboard limiter phase ($\delta t = 12s$) of about $3 \cdot 10^{22}\mathrm{Dm}^{-2}$, ensures a quasi "saturation" of the surface by deuterium and provides the necessary reservoir of D in the Be matrix to enable the above described chemically assisted physical sputtering. Present ERO modelling assumes a constant deuterium content of 50% in the thickness of the interaction matrix used in the code. This is a simplification to the really complex situation with regard to the pulsed operation of JET.

5.2 THE ROLE OF THE DEUTERIUM CONTENT IN BE ON THE SPUTTERING

Indeed experiment I, used to determine the composition of the sputtered Be, represents a complex process sequence of (i) high flux deuterium loading of Be, (ii) implantation of D in Be in different vacancies and trap sites. In parallel, (iii) the Be limiter temperature increases during the deuterium loading varying the populated vacancies and traps, and (iv) outgassing during the discharge (e.g. in figure 2 when the contact point changes from inboard to outboard) takes place as well as (v) post-discharge outgassing at elevated temperature. In fact the ratch-up of the T_{base} from one discharge to the next discharge represents a poor way of thermal desorption with stepwise increase of the desorption temperature at almost constant hold times for about $20min$ equivalent to the time between two discharges. In parallel to this temporal variation of the deuterium content in the Be PFCs, which takes place intraand inter-discharge, the observed Be sputtering via physical and chemical assisted physical sputtering takes place. As discussed before in sec. 3, the sputtering via BeD and associated production of D out of the molecular dissociation, and the increase of D_2 desorption is anti-reciprocal until almost all BeD is vanished. Thus, with respect to the amount of deuterium released by thermal desorption or as deuterium break-up product of chemical assisted physical sputtering, both processes are interconnected to the amount of D in the Be matrix populated in vacancies and traps. The reference amount of D measured spectroscopically by Balmer radiation at the limiter is almost constant for all discharges, indicating that the net amount of released deuterium remains constant in this series of discharges.

Comparison with laboratory experiments dealing with deuterium retention and release in Be is only qualitatively possible due to the large difference in the impinging flux ($\simeq 10^{17} Ds^{-1} m^{-2}$) and fluence ($\simeq 10^{22} Dm^{-2}$) in comparison to JET conditions described before including the complex loading and outgassing. In [22], dedicated studies at (a) low surface temperature ($T_{surf} = 100°C$), below the starting temperature of the Be tile observed here at JET, and at (b) high surface temperature ($T_{surf} = 280°C$) were carried out. Dedicated thermal desorption revealed in case (a) six trap sites, the two low energetic ones are related to supersaturation which vanishes with temperature as demonstrated in case (b). Two other trap sites at about ($T_{surf} = 430°C$) are only populated significantly at higher loading temperatures and have been attributed to an amorphous state which can induce direct release of BeD or BeD_2 till full thermal decomposition of the molecular species sets in [12], leaving a very narrow temperature window for the molecular release via BeD or BeD_2. Though the conditions in the laboratory studies and the tokamak experiment are different, we can exclude that the observed spectroscopic *BeD* emission in JET is attributed to a thermal desorption process via the volatile molecule BeD_2 and subsequent dissociation into *BeD*. *BeD* is most prominent at the lowest surface temperatures at JET and almost absent at the temperature window where the release according to the laboratory results shall be strongest. Therefore, we conclude that chemical assisted physical sputtering is the origin of the observed *BeD* emission and the increased sputtering yield with respect to ordinary Be sputtering as it can be calculated by TRIM for impact energies as present in the limiter plasmas.

5.3 CONCLUSIONS FOR ITER PREDICTIONS

The current experiments at JET give only limited access to different impinging flux or surface temperature conditions, but it provides overall the closest conditions with respect to ITER and can be used for direct ITER predictions with respect to erosion yields and for code benchmarking. Considering the factor 2.5 larger erosion found in the most optimistic set of input atomic and surface data (ERO_{min} in ERO simulations of the JETILW experiments), the lifetime of the first wall in ITER is longer by the same factor than current published predictions [8]. Chemical assisted physical sputtering in ERO has not yet been considered, but the bare *BeII* emission of different transitions has been used as critical benchmark with JET. Therefore, further detailed studies with variation of a single parameter, i.e change of the Be surface temperature, the impact energy of deuterons down to the predicted threshold energy, and the impinging flux, would be required to further improve the modelling input and the ITER predictions.

ACKNOWLEDGEMENTS

This work was carried out within the framework of EFDA, the Forschungszentrum Jlich and the US DOE Contract: DE-FG02-07ER54912. The views and opinions expressed herein do not necessarily reflect those of the European Commission.

REFERENCES

[1]. V. Philipps et al.; Fusion Engineering and Design **85** (2010) 1581–1586
[2]. S. Carpentier et al., Journal of Nuclear Materials **415** (2011) S165
[3]. D. Borodin et al., Physica Scripta **T145** (2011) 14008
[4]. G.F. Matthews et al., Journal of Nuclear Materials **438** (2013) S2
[5]. S. Brezinsek et al., Journal of Nuclear Materials **438** (2013) S303
[6]. S. Brezinsek et al., Nuclear Fusion **53** (2013) 083023
[7]. J.W. Coenen et al., Nuclear Fusion **53** (2013) 073043
[8]. G.F. Matthews et al., Physica Scripta **T145** (2011) 014011
[9]. G. Duxbury et al., Plasma Physics and Controlled Fusion **40** (1998) 361
[10]. S. Brezinsek et al., ECA **37D** (2013)
[11]. W. Eckstein et al., Report IPP **9/132** (2002)
[12]. D. Nishijima et al., Plasma Physics and Controlled Fusion **50** (2009) 125007
[13]. D. Borodin et al., Journal of Nuclear Materials **438** (2013) S267
[14]. R.P. Doerner et al., Journal of Nuclear Materials **390–391** (2009) 681
[15]. ADAS, http://adas.phys.strath.ac.uk
[16]. P.C. Stangeby, The plasma boundary of magnetic fusion devices, IOP publishing (2000)
[17]. G. Arnoux et al., Nuclear Fusion **53** (2013) 073016
[18]. S. Brezinsek et al., Plasma Physics and Controlled Fusion **47** (2005) 615
[19]. S. Brezinsek et al., Journal of Nuclear Materials **363–365** (2007) 1119

[20]. C. Björkas et al., New Journal of Physics **11** (2009) 123017
[21]. A. Widdowson et al., accepted for Physica Scripta
[22]. M. Reinelt et al., New Journal of Physics **9** (2009) 043023

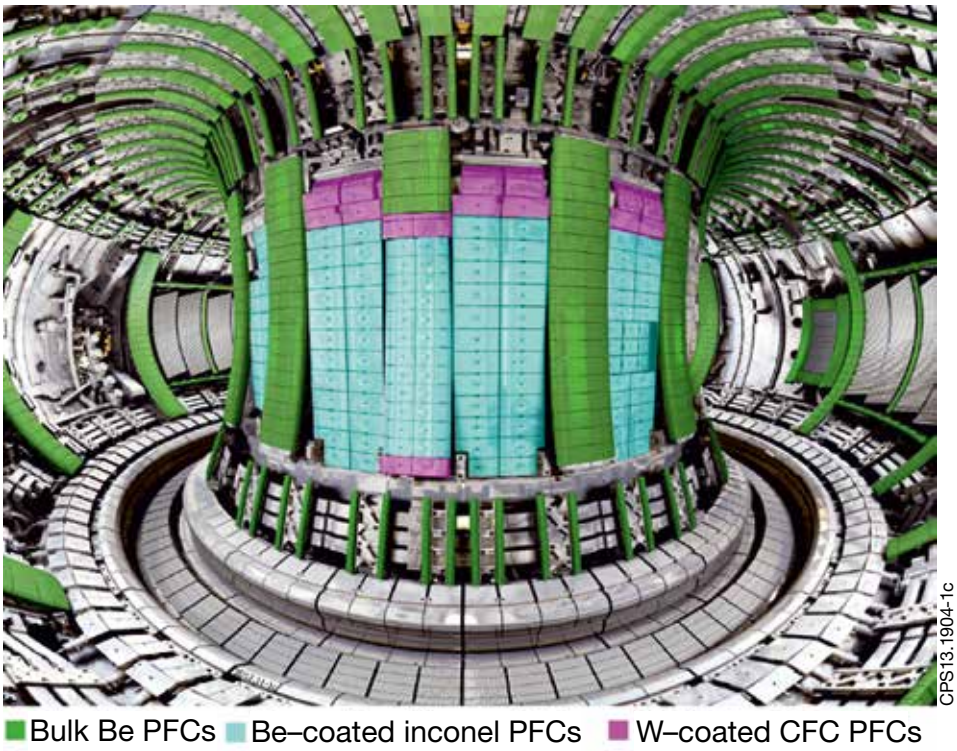

Figure 1: The JET ITER-Like Wall: Bulk Be (Brush Wellman grade S65J HIP) PFCs are installed at the low and high-field side as main limiter. Be-coated inconcel tiles are used as cladding of the main chamber wall. W-coated CFC is introduced at specific areas of high power impact (NBI shinethrough areas, Re-ionisation tiles etc. [8]).

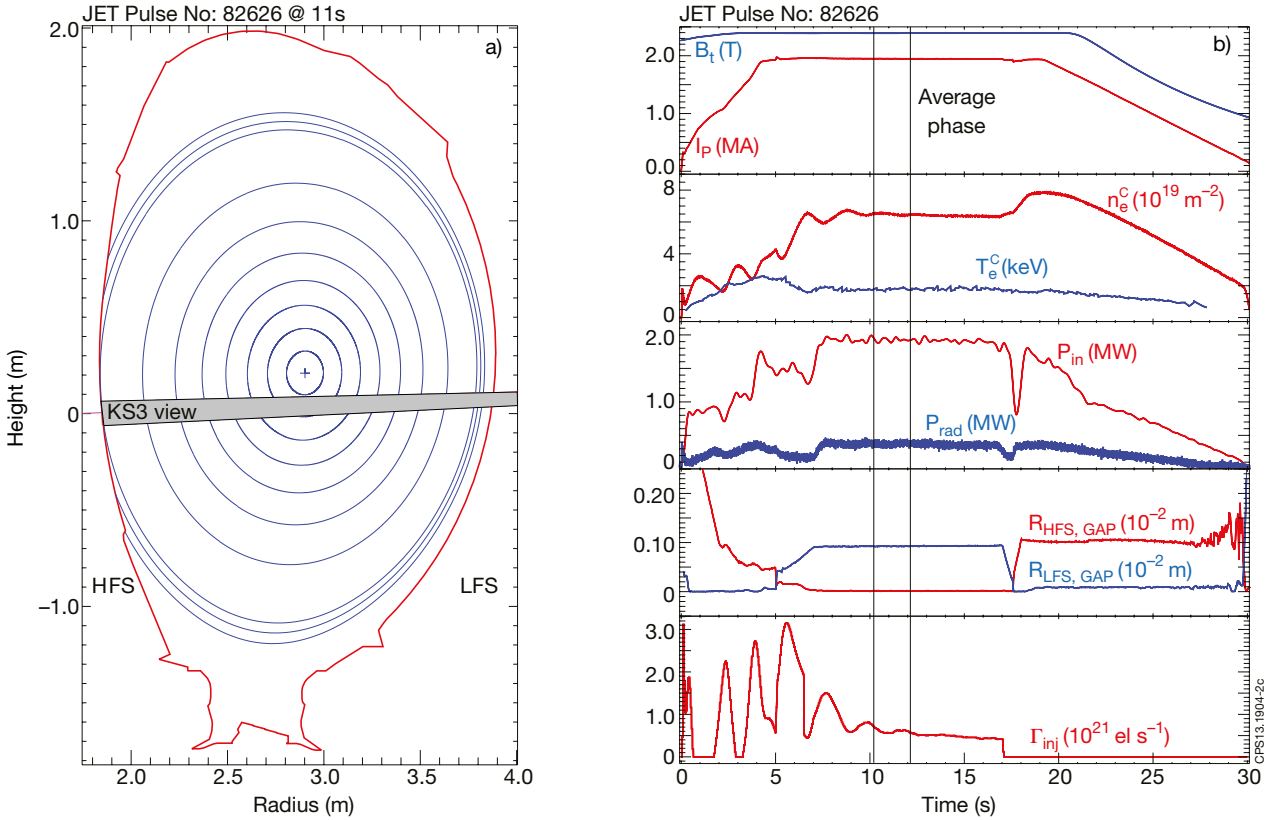

Figure 2: a) Applied limiter shape in the experiments. b) Evolution of global parameters for the last discharge of experiment (I) [JET Pulse No: 82592 – 82626].

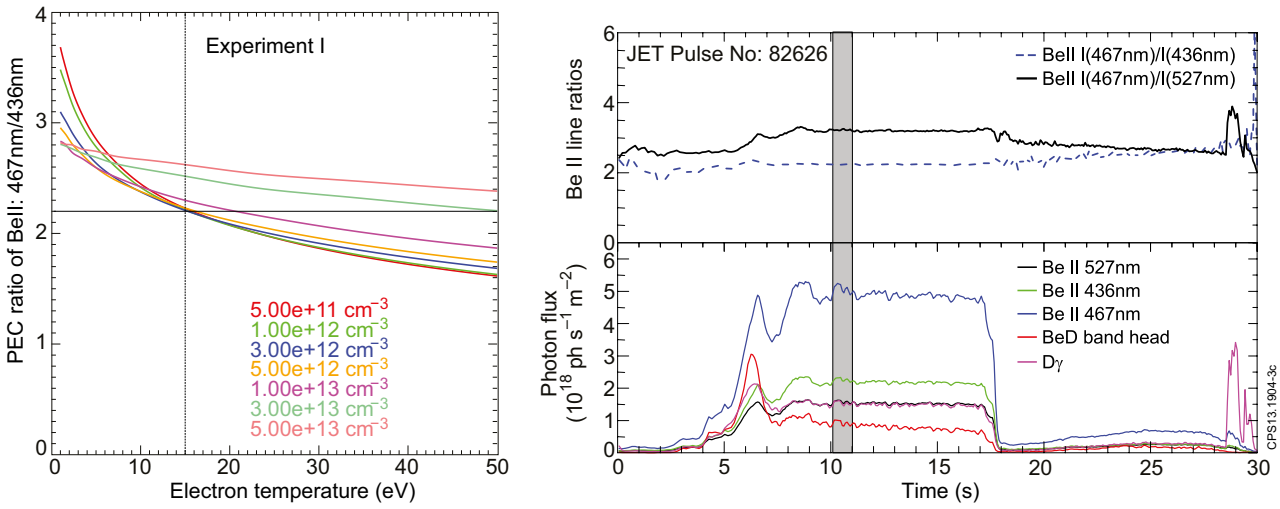

Figure 3: a) Ratio of photon emission coeffcients of BeII for the transitions at 467nm and 436nm from ADAS. b) Temporal evolution of three different BeI I lines and the corresponding line ratios for discharge 82626.

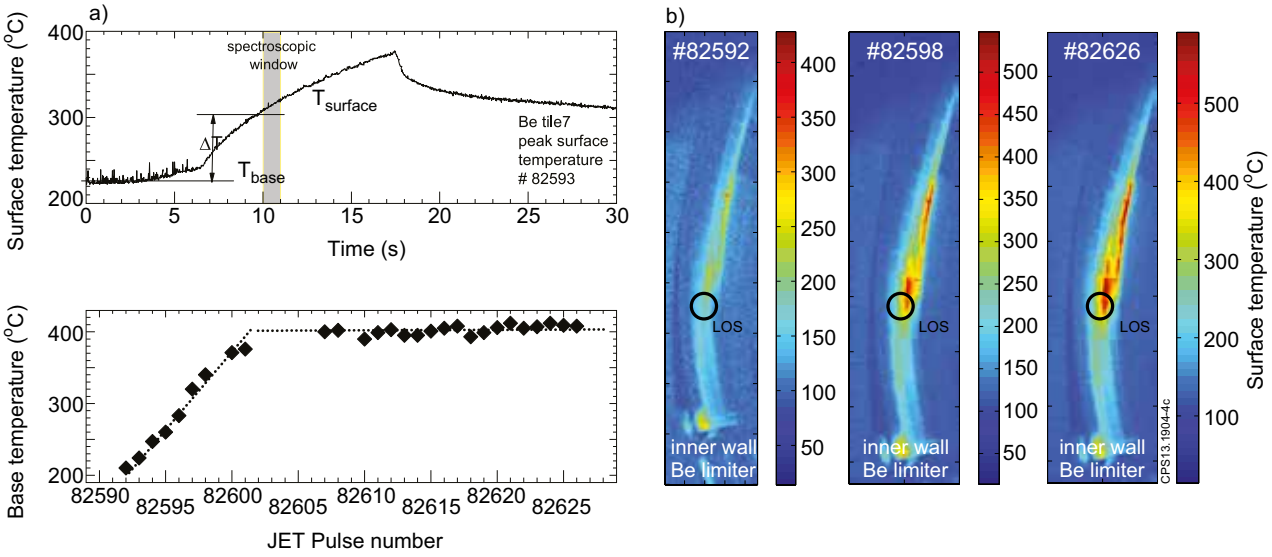

Figure 4: a) Top: Temperature evolution of the observed Be tile in one discharge. Bottom: Temperature evolution of the observed Be tile in all discharges of experiment (i). b) 2D distribution of the temperature on the inner wall Be limiters for three dedicated discharges of the series of 34 identical plasmas in experiment (i) [JET Pulse No: 82592 – 82626].

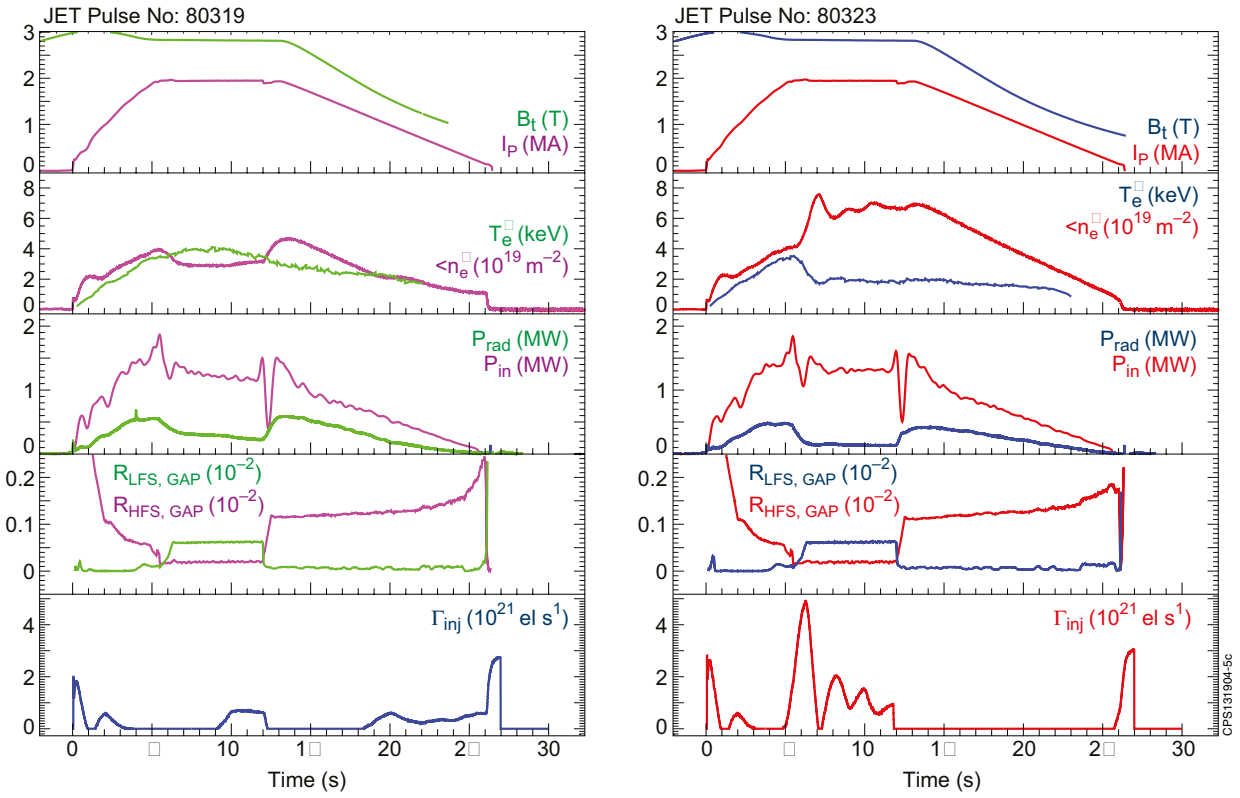

Figure 5: Timetraces of global plasma parameters of discharges in limiter configuration at lowest (a: JET Pulse No: 80319) and highest fuelling level (b: JET Pulse No: 80323) used to vary the impact energy Ein of deuterons at the limiter contact point.

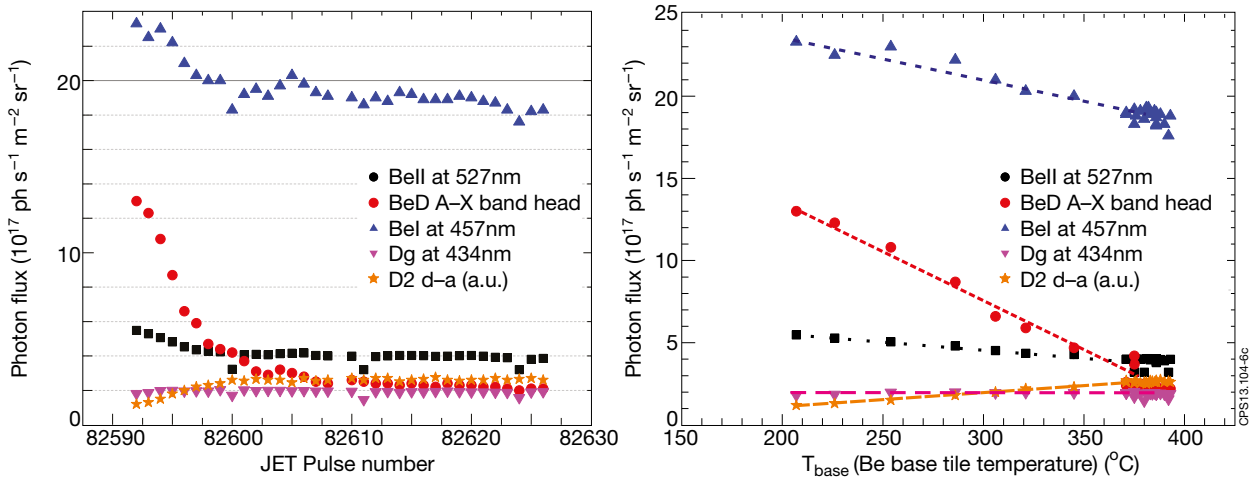

Figure 6: Experiment (i): a) Discharge to discharge evolution of Be and D photon fluxes with constant plasmas. b) Photon flux evolution of the different species as function of the base temperature of the bulk Be tile 7.

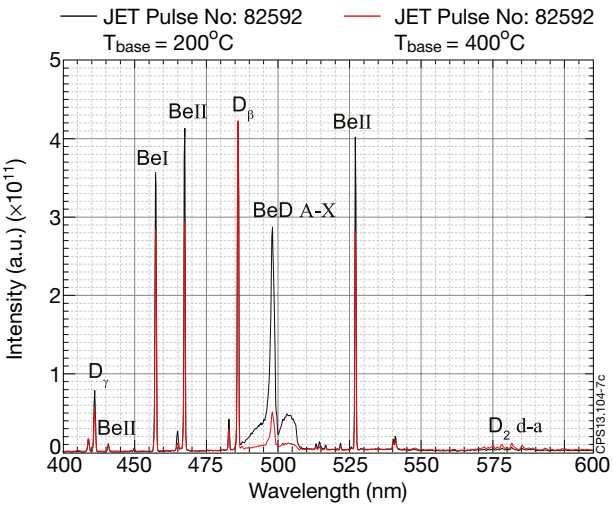

Figure 7: Emission spectra recorded at the Be limiter at the first and last discharge of the series in experiment I representing low T_{base} [JET Pulse No: 82592] and high T_{base} [JET Pulse No: 82626] conditions.

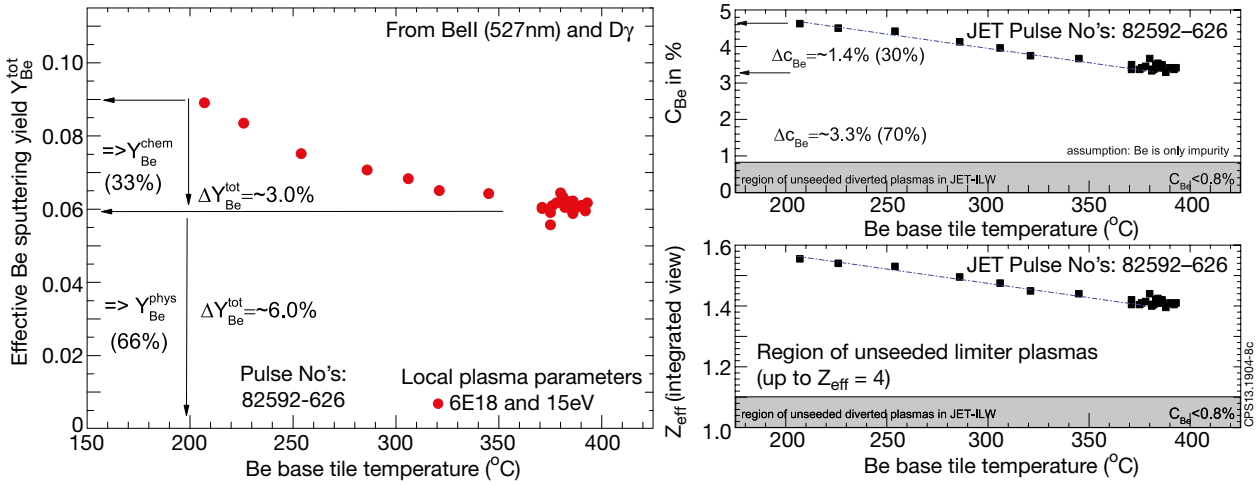

Figure 8: Experiment (i): a) Contributors to Y^{tot}_{Be} as function of T_{base} . b) Variation of c_{Be} with T_{base}. c) Variation of Z_{eff} with T_{base}.

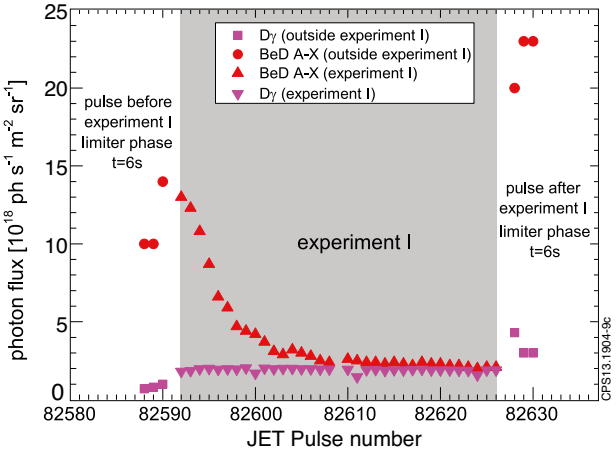

Figure 9: Appearance of BeD A-X emission in the short limiter start-up phase of three discharges directly prior and post the series of experiment I discharges.

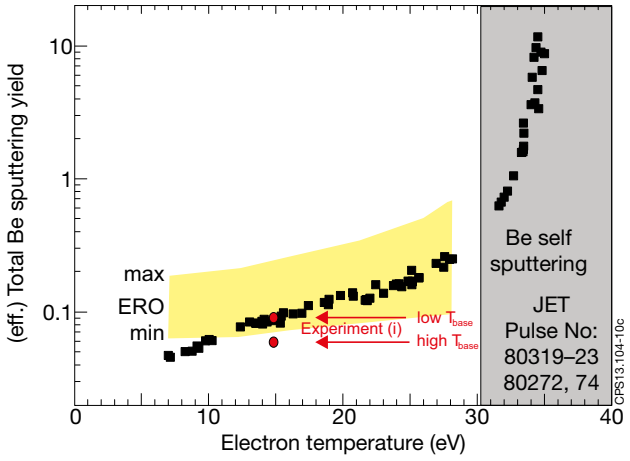

Figure 10: Y_{Be}^{tot} as function of the local T_e or $^1/_5\,E_{in}$ in experiment (ii). The shadowed area indicated ERO modelling with the compiled sputtering data ERO_{max} and ERO_{min} for the bare physical sputtering yields [8].

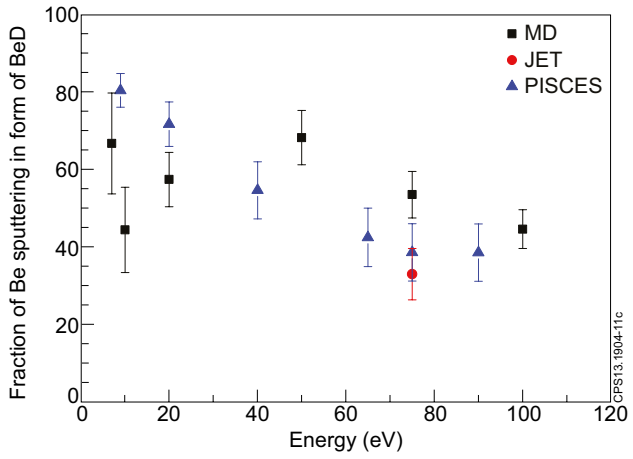

Figure 11: Fraction of total Be sputtering released as BeD in JET, PISCES and MD calculations as function of impact energies of deuterons. The variation in the low energy end of the MD calculations is caused by low statistics in the overall small sputtering yield.